Journal of Statistical Physics, Vol. 66, Nos. 3/4, 1992

Velocity Spectrum for Non-Markovian Brownian Motion in a Periodic Potential

A. Igarashi,[1] P. V. E. McClintock,[2] and N. G. Stocks[2]

Received June 21, 1991

Non-Markovian Brownian motion in a periodic potential is studied by means of an electronic analogue simulator. Velocity spectra, the Fourier transforms of velocity autocorrelation functions, are obtained for three types of random force, that is, a white noise, an Ornstein–Uhlenbeck process, and a quasimonochromatic noise. The analogue results are in good agreement both with theoretical ones calculated with the use of a matrix-continued-fraction method, and with the results of digital simulations. An unexpected extra peak in the velocity spectrum is observed for Ornstein–Uhlenbeck noise with large correlation time. The peak is attributed to a slow oscillatory motion of the Brownian particle as it moves back and forth over several lattice spaces. Its relationship to an approximate Langevin equation is discussed.

KEY WORDS: Analog simulation; non-Markovian process; periodic potential; velocity spectrum; colored noise; Brownian motion; Langevin equation; matrix-continued-fraction method.

1. INTRODUCTION

Brownian motion in a periodic potential has been widely studied in many branches of physics and chemistry, for example, as a model of the diffusive motion of impurities in crystals, the motion of ions in superionic conductors, chemical reactions, and so on.[1–7,11] Non-Markovian effects for Brownian motion have recently been investigated by many workers.[7–15] In a previous paper,[1] one of the authors (A.I.) investigated the escape rate from a potential well and velocity autocorrelation functions for this model theoretically by use of the matrix-continued-fraction (MCF) method,[2,4]

[1] Department of Applied Mathematics and Physics, Kyoto University, Kyoto 606, Japan.
[2] School of Physics and Materials, University of Lancaster, Lancaster, LA1 4YB, United Kingdom.

0022-4715/92/0200-1059$06.50/0

and compared non-Markovian effects for the three kinds of random force. As mentioned in ref. 1, however, it becomes very difficult to calculate the velocity spectrum for small values of the friction and other parameters theoretically from MCF because of the explosive increase of computing time and memory size required even if supercomputers can be used. Simulation is potentially a useful method to apply in cases such as this, where theories do not work well. Experiments based on analogue electronic circuits can provide a powerful method for simulating stochastic nonlinear differential equations.[16]

In this paper, non-Markovian Brownian motion in a periodic potential under the influence of colored random forces is simulared with the use of analogue electronic circuits. We consider three kinds of random force: a white noise (WN), an Ornstein–Uhlenbeck process (OU), and a quasimonochromatic noise (QMN), which have Dirac delta correlation, exponential correlation, and damped-oscillatory correlation, respectively. Hereafter, our models with the random forces of WN, OU, and QMN are called models (a), (b), and (c), respectively. Since velocity spectra (VS), that is, the Fourier transforms of the velocity autocorrelation functions of the Brownian particle, are convenient quantities to describe the characteristics of its motion, we measure and investigate them in detail.

First, we obtain VS for the parameter region in which they can be calculated theoretically with the use of MCF and compare the simulation results with theoretical ones in order to confirm the accuracy of our analogue simulation. Next, we measure the VS for the parameter range for which MCF theory does not work well. For example, the VS for model (b) with large correlation time of the random force is obtained. In this case, we discover an unexpected extra peak in the VS on the left of the usual peak corresponding to oscillation of the particle near the bottom of a potential well (which always exists in VS for the three models with arbitrary values of the parameters). This extra peak has not been observed either in model (a) or in model (b) with small correlation time of the random force. From observation of the actual motion of the particle for the above case, we see that there exist two quite different characteristic motions of the particle, that is, fast oscillation near the bottoms of potential wells and a motional pattern in which the Brownian particle goes back and forth over several lattice spaces. From these facts, we conclude that the latter type of dynamical behavior causes the new peak. We further investigate the dependence of the frequency at the peak upon the correlation time of the random force and upon the friction constant. A possible relationship between the extra peak and an approximate Langevin equation, which entirely neglects the force due to the periodic potential, is explored.

In Section 2, we specify our models for Brownian motion. Section 3

contains the description of our analogue simulation. The simulation results are analyzed in Section 4. In Section 5, the relationship between the extra peak and the approximate Langevin equation is discussed. We summarize our conclusions in Section 6.

2. NON-MARKOVIAN BROWNIAN-MOTION MODEL

We consider the non-Markovian Brownian-motion model governed by the following generalized Langevin equation:

$$M\frac{d^2x}{dt^2} = -\frac{dV(x)}{dx} - M\int_0^t ds\, K(t-s)\cdot\frac{dx(s)}{ds} + F(t) \tag{1}$$

where $x(t)$ denotes the position of the Brownian particle with mass M and $V(x)$ is a periodic potential,

$$V(x) = \frac{E_b}{2}\left[1 - \cos\left(\frac{2\pi x}{a}\right)\right] \tag{2}$$

E_b is the amplitude of $V(x)$ with lattice constant a. The effective friction constant ζ for this system is defined by

$$\zeta = \int_0^\infty K(s)\, ds \tag{3}$$

and the fluctuation dissipation relation holds, that is,

$$\langle F(t)\, F(s)\rangle = Mk_B TK(t-s) \tag{4}$$

where k_B and T are the Boltzmann constant and temperature, respectively. $\langle A\rangle$ expresses the ensemble average of a dynamical variable A.

Three types of random force $F(t)$ are considered:

$$\text{model (a)} \quad F(t) = (\zeta Mk_B T)^{1/2} f(t) \tag{5}$$

$$\text{model (b)} \quad \frac{dF(t)}{dt} = -\gamma F(t) + (\gamma^2 \zeta Mk_B T)^{1/2} f(t) \tag{6}$$

$$\text{model (c)} \quad \frac{d^2F(t)}{dt^2} = -\Omega^2 F(t) - \xi\frac{dF(t)}{dt} + (\Omega^4 \zeta Mk_B T)^{1/2} f(t) \tag{7}$$

The $f(t)$ denotes white noise whose correlation is

$$\langle f(t)\, f(s)\rangle = 2\delta(t-s) \tag{8}$$

For model (a), $F(t)$ is a white noise process (WN). Since $F(t)$ has the Dirac delta correlation, $K(t)$ is, from (4) and (5), given by,

$$K(t) = 2\zeta\delta(t) \tag{9}$$

The random force for model (b) is an Ornstein–Uhlenbeck process (OU), which has exponential correlation. From (4) and (6), we have

$$K(t) = \zeta\gamma e^{-\gamma|t|} \tag{10}$$

In model (c), the Brownian particle is influenced by a quasimonochromatic noise (QMN) in which the random force has a damped oscillatory correlation. With the use of (4) and (7), $K(t)$ is expressed by

$$K(t) = \frac{\Omega^2\zeta}{\xi}\exp\left(-\frac{\xi|t|}{2}\right)\left[\cos(\omega_1 t) + \frac{\xi}{2\omega_1}\sin(\omega_1|t|)\right] \tag{11}$$

with $\omega_1 = (\Omega^2 - \xi^2/4)^{1/2}$.

In model (a), (1) is rewritten as a first-order simultaneous stochastic differential equation as follows:

$$\begin{aligned} \dot{x} &= v \\ \dot{v} &= -\zeta v - \frac{1}{M}\frac{dV(x)}{dx} + \left(\frac{\zeta k_B T}{M}\right)^{1/2} f(t) \end{aligned} \tag{12}$$

where v denotes the velocity of the particle. From (12), we see that $(x, v = \dot{x})$ is a Markovian process with two variables in model (a). On the other hand, $(x, v = \dot{x})$ does not constitute a Markovian process in models (b) and (c). These models can be regarded, however, as being Markovian, if we introduce some additional variables. For model (b), introducing an additional variable z, we can transform the Langevin equation (1) to

$$\begin{aligned} \dot{x} &= v \\ \dot{v} &= -\frac{1}{M}\frac{dV(x)}{dx} + z \\ \dot{z} &= -\gamma\zeta v - \gamma z + \left(\frac{\zeta\gamma^2 k_B T}{M}\right)^{1/2} f(t) \end{aligned} \tag{13}$$

Then, (x, v, z) is a Markovian process with three variables. Finally, model (c) becomes a Markovian process with four variables, x, v, z, w. That is,

$$\begin{aligned}
\dot{x} &= v \\
\dot{v} &= -\frac{1}{M}\frac{dV(x)}{dx} + z \\
\dot{z} &= -\frac{\Omega^2\zeta}{\xi} v + w \\
\dot{w} &= -\xi w - \Omega^2 z + \left(\frac{\zeta\Omega^4 k_B T}{M}\right)^{1/2} f(t)
\end{aligned} \tag{14}$$

The matrix-continued-fraction (MCF) method[2,4] can be applied to the above three models as reported in ref. 1. From MCF, the velocity spectrum (VS) $\phi(\omega)$, defined by

$$\phi(\omega) = \int_{-\infty}^{\infty} dt\, e^{-i\omega t} \langle v(t)\, v(0) \rangle \tag{15}$$

can readily be obtained for relatively large values of the parameters ζ, γ, ξ, and Ω.

In the next section, we describe how to simulate these three models with analogue electronic circuits and thus obtain $\phi(\omega)$.

3. ANALOGUE SIMULATION

Our systems are simulated by electronic circuits. For example, a schematic diagram of model (b) is shown in Fig. 1. The white noise is obtained from a Wandel & Golterman model RG1 noise generator, which produces an accurately Gaussian noise voltage with a flat frequency response over the band range 0–100 kHz. Before application to the circuit, the noise is filtered through a low-pass filter. This ensures that the noise has a well-defined correlation time, which is set to be much smaller than the time constant of the circuit. The voltage summation, integration, inversion, and amplification are accomplished by standard operational amplifiers, while the trigonometric function is performed by commercially available integrated circuits. We have to simulate our systems within two

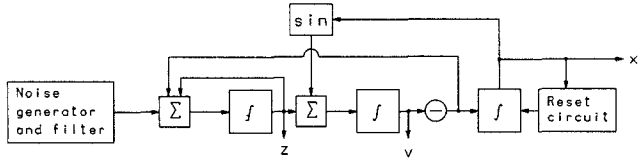

Fig. 1. Schematic diagram of the electronic circuit used for model (b).

cycles of the potential, however, since the integrated circuit realizes its trigonometric function only over about two cycles. Consequently, a reset circuit is required to bring the Brownian particle back to the equivalent point in the periodic potential within the region available for the integrated circuit, whenever it would otherwise leave this region. The reset circuit is not shown in detail, but its operation is straightforward. A pair of voltage comparators is operated at the output of x, and they are immediately triggered to drive $x \to 0$ V when x exceeds the boundary. It is obviously essential that the resetting process should be achieved within a time that is small compared to any other time scale of importance in the simulation. The output voltage from the circuit corresponding to $v(t)$ is analyzed by means of a digital data processor (Nicolet LAB80) and $\phi(\omega)$ is obtained by application of a standard fast Fourier transform (FFT) algorithm.

4. SIMULATION RESULTS

In this section, we present our simulation results for $\phi(\omega)$. We choose a, E_b, and $1/\omega_0 = 1/(2\pi^2 E_b/Ma^2)^{1/2}$ as units of length, energy, and time, respectively, that is, $T^* = k_B T/E_b$, $\zeta^* = \omega_0 \zeta$, etc.

In Fig. 2, $\phi(\omega)$ for models (a) and (b) obtained from analogue simulation is shown and compared with theoretical results obtained by the use of MCF. In this figure, we choose $T^* = 0.5$ and $\zeta^* = 1.0$, and $\gamma^* = 1.0$ for

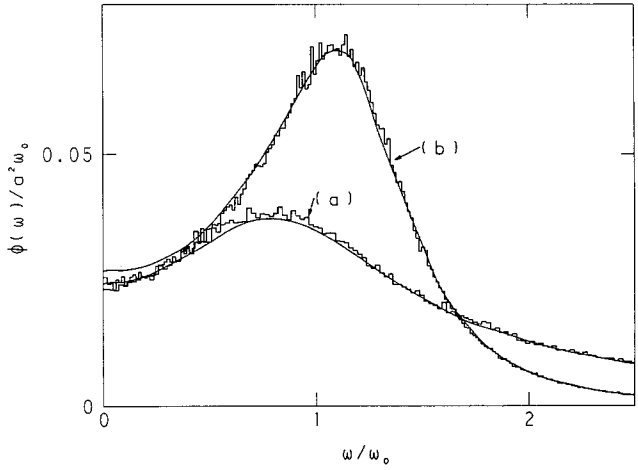

Fig. 2. Velocity spectra $\phi(\omega)$ obtained from analog simulation (zigzag lines) and from the MCF method (smooth lines). (a) Model (a) with $T^* = 0.5$ and $\zeta^* = 1.0$; (b) model (b) with $T^* = 0.5$, $\zeta^* = 1.0$, and $\gamma^* = 1.0$. The simulation and theoretical results are evidently in good agreement with each other.

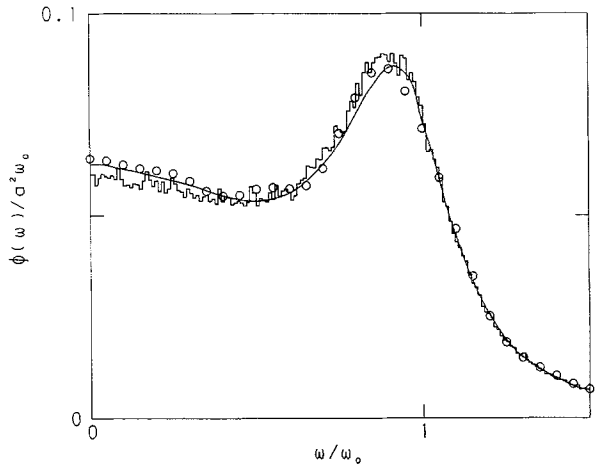

Fig. 3. Velocity spectra $\phi(\omega)$ for model (b) with $T^*=0.5$, $\zeta^*=0.25$, and $\gamma^*=1.0$. The smooth line denotes the results from MCF, the zigzag line that from analogue simulation, and the circles that from digital simulation. The three results are in good agreement with each other.

model (b), and find that each curve has one peak. These peaks are due to the oscillatory motion near the minima of the potential. Theoretical results agree with simulation results quite well. Figure 3 shows $\phi(\omega)$ for model (b) with $T^*=0.5$, $\zeta^*=0.25$, and $\gamma^*=1.0$. The analogue simulation results are compared with theoretical results and digital simulation results. In the

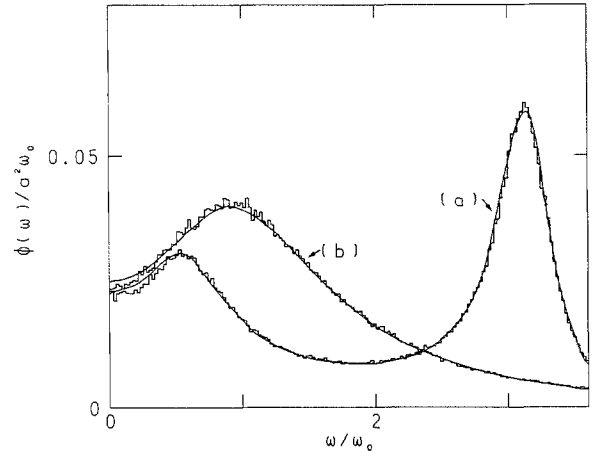

Fig. 4.. Velocity spectra obtained from analog simulation (zigzag lines) and from the MCF method (smooth lines). (a) $\phi(\omega)$ for model (c) with $T^*=0.5$, $\zeta^*=1.0$, $\xi^*=1.0$, and $\Omega^{*2}/\xi^*=5.0$; (b) that for model (b) with $T^*=0.5$, $\zeta^*=1.0$, and $\gamma^*=5.0$. Agreement between simulation and theoretical results is quite good.

latter figure, the peak of $\phi(\omega)$ corresponds to oscillations near the bottoms of potential wells. The three results are almost coincident with each other. The $\phi(\omega)$ for model (c) with $T^* = 0.5$, $\zeta^* = 1.0$, $\xi^* = 1.0$, and $\Omega^{*2}/\xi^* = 5.0$ and that for model (b) with $T^* = 0.5$, $\zeta^* = 1.0$, and $\gamma^* = 5.0$ are depicted in Fig. 4, and analogue simulation results are compared with theoretical ones. In this figure, two peaks can be observed in $\phi(\omega)$ for model (c). The left one corresponds to the peaks in Figs. 2 and 3, and the right one is due to the frequency of the random force. In Fig. 4, theoretical results are in good agreement with simulation ones. From these results shown in Figs. 2–4, we confirm the accuracy of our analogue simulation.

Next, we simulate model (b) with a small value of γ, since MCF theory does not work well in the region of small parameters. The result is shown in Fig. 5, where T^*, ζ^*, and γ^* are specified to be 0.5, 1.0, and 0.1, respectively. From Fig. 5, we see that *two* peaks appear in the $\phi(\omega)$ curve. To make absolutely certain, we recalculated $\phi(\omega)$ with the use of a digital computer, the difference scheme for our digital simulation being similar to that used in ref. 7. The result is compared with the analogue simulation measurements in Fig. 5. The agreement between the two results is quite good. The right peak is due to the oscillatory motion near the bottoms of the potential. The left peak is an extra new one and was quite unexpected, because the random force in model (b) has no characteristic frequencies of its own, unlike that in model (c). This extra peak exists for model (b) with

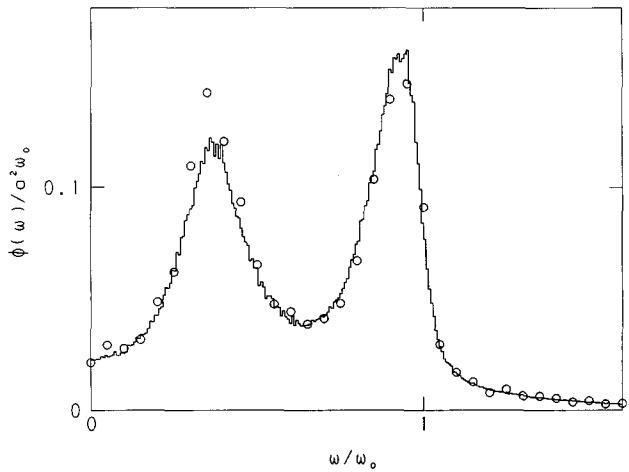

Fig. 5. Velocity spectra obtained from analogue (curve) and digital (circles) simulation. T^*, ζ^*, and γ^* are specified to be 0.5, 1.0, and 0.1, respectively. Analogue and digital simulation results are in good agreement with each other and confirm the reality of the additional peak at low frequencies.

$\gamma^* < 0.8$ and $\zeta^* < 10.0$. The smaller γ or ζ becomes, the lower and the broader the shape of the extra peak becomes. In order to demonstrate the physical origin of this extra peak, $v(t)$ and $x(t)$ measured for the same values of parameters as in Fig. 5 are depicted in Fig. 6. We see immediately that the Brownian particle has two quite distinct characteristic motional patterns. The one which appears on the right-hand side of this figure represents oscillatory motion near the bottom of a potential well and the other, which appears in the extreme left and center parts of the figure, is a slower motion corresponding to the particle moving back and forth over several lattice spaces. These two characteristic motional patterns exist universally for model (b) in the region of the parameters in which $\phi(\omega)$ has the extra peak. This slow motion has not been observed at all for model (a), or for model (b) or (c) with parameter values chosen as in Figs. 2–4. We have investigated how the position of this extra peak depends on the values of γ and ζ. When the correlation time of the random force $1/\gamma$ decreases, the extra peak is found to shift to the right, finally disappearing for about $\gamma^* = 0.8$. It relates to a decrease in the period of the slow oscillation because the correlation time of motion decreases with a decrease in the correlation time of the random force. When the effective friction constant ζ increases, the peak is found to shift toward the right, finally merging into the right peak for about $\zeta^* = 10.0$. The reason for this is that the period of

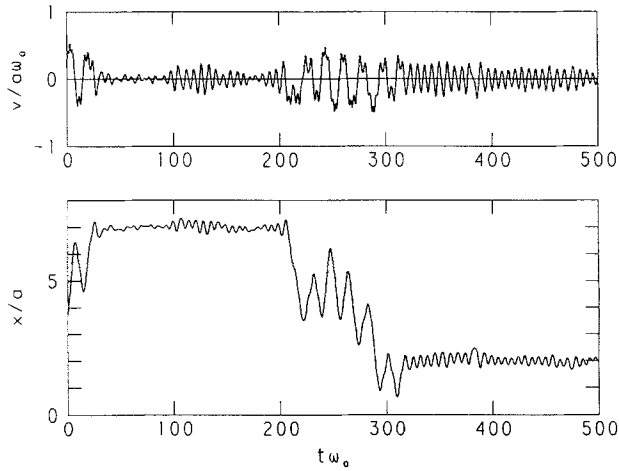

Fig. 6. The velocity and position of the Brownian particle of model (b) with the same parameter values as in Fig. 5, plotted as a function of time in the same time interval. Two characteristic motional patterns are observed in this figure. The one on the right represents the oscillation of the particle near the bottom of a potential well, and the other, which is on the extreme left and middle, corresponds to slow oscillatory motion as the particle goes back and forth over several lattice spaces.

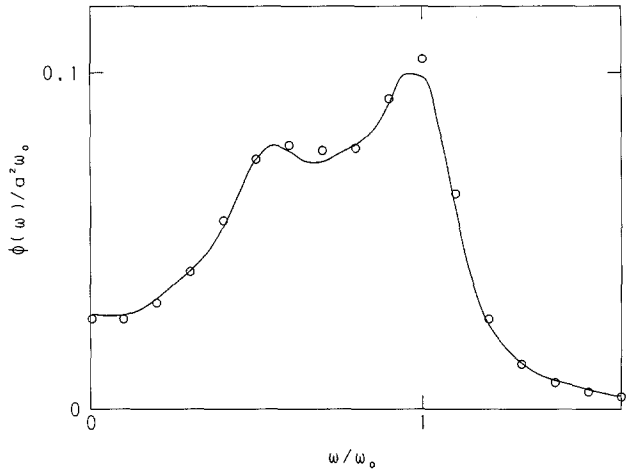

Fig. 7. The velocity spectrum $\phi(\omega)$ for model (b) with $T^*=0.5$, $\zeta^*=1.0$, and $\gamma^*=0.25$ obtained from digital simulation, compared with theoretical results from MCF (circles). The MCF theory reproduces the simulation results quite well.

the slow motion becomes long as a result of increasing the decay time of motion due to the decrease of the effective friction constant.

Finally, in order to obtain further confirmation of the existence of the extra peak, $\phi(\omega)$ for model (b) with $T^*=0.5$, $\zeta^*=1.0$, and $\gamma^*=0.25$ was computed by the use of MCF. (Since MCF cannot be applied for the parameters employed in Fig. 5 and 6 because of the prohibitive length of computing time that would be required, we were obliged to choose a slightly larger value of γ.) In Fig. 7, we compare the theoretical results with those from a digital simulation. They are clearly in good agreement with each other, so that the reality of the additional peak in the velocity spectrum cannot be in doubt.

5. DISCUSSION

H. Risken has made an interesting suggestion to try to account for the new peak. He points out[17] that, if the force due to the periodic lattice is neglected in (13), one then obtains a linear Langevin equation in v,

$$\frac{d^2v}{dt^2}=-\gamma\zeta v-\gamma\frac{dv}{dt}+\left(\frac{\zeta\gamma^2k_BT}{M}\right)^{1/2}f(t) \tag{16}$$

For suitably chosen parameter values, the velocity spectrum corresponding to (16) *exhibits a peak*, and it seems plausible that the latter might be related to the additional peak found in the VS of (13). Following this

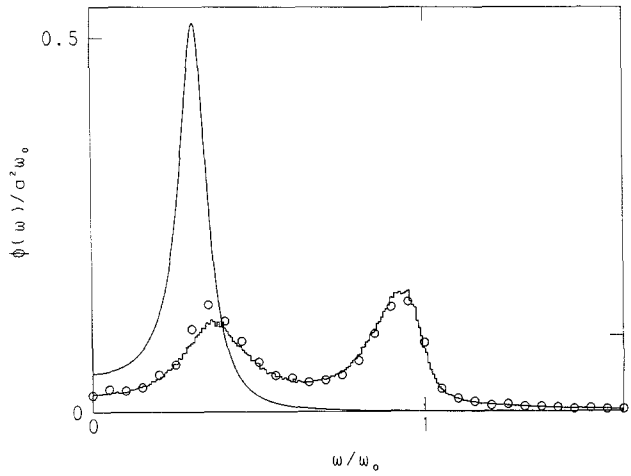

Fig. 8. The velocity spectrum $\phi(\omega)$ for (16) (smooth curve) compared with that for (13) obtained from analog (zigzag curve) and digital (circles) simulation. T^*, ζ^*, and γ^* are specified to be the same values as in Fig. 5.

suggestion, we have calculated VS of the approximate equation (16): an example, for the same set of parameters as those of Fig. 5, is shown (smooth curve) in Fig. 8 and compared with the analogue and digital results from (13). It is evident that the positions of the peaks are in quite good agreement, but their magnitudes and widths differ. The latter discrepancies are not at all surprising, however, given the gross approximation inherent in our complete neglect of the periodic potential in the derivation of (16). It is interesting to note that the dynamics giving rise to the new peak, in which the particle gains sufficient energy to move freely across several lattice spaces (see above), represents the classical analogue of a Bloch wave in the periodic potential of a crystal.

6. CONCLUSION

We have simulated a non-Markovian Brownian-motion model in a periodic potential with the aid of analogue electronic circuits, and have compared the simulation results with theoretical predictions based on the use of MCF for large parameter values. The good agreement between them confirms the accuracy of our simulation technique. In the case of model (b) with a large correlation time of the random force, an extra new peak has been discovered and shown to be closely related to a slow oscillatory motion in which the particle goes back and forth across several lattice

spaces. The existence of this extra peak may be accounted for semiquantitatively in terms of an approximate Langevin equation in which the effect of the periodic potential is ignored.

ACKNOWLEDGMENTS

It is a pleasure to thank Prof. H. Risken of Ulm University, and an anonymous referee, for valuable comments on an earlier version of Section 5. This work was supported by the Science and Engineering Research Council (U.K.) and by the Japanese Ministry of Education. One of the authors (A.I.) would like to acknowledge the welcome hospitality of Lancaster University.

REFERENCES

1. A. Igarashi and T. Munakata, *J. Phys. Soc. Jpn.* **57**:2439 (1988).
2. H. Risken, *The Fokker–Planck Equation: Methods of Solution and Applications*, 2nd ed. (Springer-Verlag, Berlin, 1989), Chapters 10 and 11.
3. W. Dieterich, I. Peschel, and W. R. Schneider, *Z. Phys. B* **27**:177 (1977).
4. H. Risken and H. D. Vollmer, *Z. Phys. B* **33**:297 (1979).
5. W. Dieterich, P. Fulde, and I. Peschel, *Adv. Phys.* **29**:527 (1980).
6. S. M. Soskin, *Physica A* **155**:401 (1989).
7. T. Munakata and T. Kawakatsu, *Prog. Theor. Phys.* **74**:262 (1985); T. Munakata, *Prog. Theor. Phys.* **75**:747 (1986).
8. S. H. Northrup and J. T. Hynes, *J. Chem. Phys.* **73**:2700 (1980).
9. R. F. Grote and J. T. Hynes, *J. Chem. Phys.* **73**:2715 (1980).
10. P. Hänggi and F. Mojtabai, *Phys. Rev. A* **26**:1168 (1982).
11. R. F. Grote and J. T. Hynes, *J. Chem. Phys.* **77**:3736 (1982).
12. B. Carmeli and A. Nitzan, *Phys. Rev. A* **29**:1481 (1984).
13. T. Munakata, *Prog. Theor. Phys.* **73**:826 (1985).
14. J. E. Straub, M. Borkovec, and B. J. Berne, *J. Chem. Phys.* **84**:1788 (1986).
15. F. Marchesoni and P. Grigolini, *J. Chem. Phys.* **78**:6287 (1983).
16. P. V. E. McClintock and F. Moss, in *Noise in Nonlinear Dynamic Systems*: Vol. 3, *Experiments and Simulations*, F. Moss and P. V. E. McClintock, eds. (Cambridge University Press, Cambridge, 1989), Chapter 9.
17. H. Risken, private communication.